PHYSICAL REVIEW A VOLUME 39, NUMBER 12 JUNE 15, 1989

Method for calculating Auger decay rates in molecules

Renato Colle and Stefano Simonucci
Scuola Normale Superiore, 56100 Pisa, Italy
(Received 3 January 1989)

A new method for calculating Auger decay rates in molecules is proposed and tested. Essential features are (1) construction of the continuum orbital via solution of the Lippmann-Schwinger equation with a projected potential, (2) matching in the asymptotic region of the Lippmann-Schwinger wave function with the eigenfunctions of the long-range Hamiltonian, and (3) complete evaluation of the Auger matrix elements between Hartree-Fock wave functions for the initial and final states. The method is tested on the *KLL* Auger spectrum of atomic Ne and then used to predict Auger decay rates for the LiF molecule ionized in its deepest shell.

I. INTRODUCTION

The importance of the Auger effect—from both experimental and theoretical points of view—and the lack of quantitative predictions, from first principles, of the Auger decay rates in molecules and solids, provide a strong incentive for developing accurate methods for the *ab initio* calculation of such decay rates.

While the general theory for treating resonant scattering problems of this type has been developed,[1] the existing predictions of experimental linewidths refer mostly to atomic systems, since the presence of a nonspherical potential inside a molecule hinders the use of standard numerical techniques. Approaches based on expansions in terms of basis functions require the solving of problems like the proper description of the continuum orbital both in the molecular and in the asymptotic region, and the evaluation of polycentric bound-free integrals for the transition matrix elements. Ways which have been suggested in the past to overcome these difficulties include the use of monocentric expansions for the potential and the continuum orbital [hence applicable only to atomlike molecules, e.g., hydrogen fluoride (Refs. 2–4)], simple approximations for the continuum orbital,[5,6] and semiquantitative estimates based on atomic decompositions.[7–9]

In this paper we present a new method for evaluating the Auger decay rates in molecules, which is characterized by the following main points.

(1) The approximate representation—in a finite discrete basis set of L^2 functions $\{\langle \mathbf{r}|\alpha\rangle\}$— of the scattering potential $\hat{V}(\mathbf{r},\{\mathbf{R}\})$, to which the outgoing electron is subjected at a given molecular geometry $\{\mathbf{R}\}$:

$$\hat{V}(\mathbf{r},\{\mathbf{R}\}) \sim \hat{V}^t(\mathbf{r},\{\mathbf{R}\}) = \sum_{\lambda,\mu,\nu,\tau} \langle \mathbf{r}|\lambda\rangle S^{-1}_{\lambda\mu} \langle \mu|\hat{V}|\nu\rangle S^{-1}_{\nu\tau} \langle \tau|\mathbf{r}\rangle \ , \qquad S_{\lambda\mu} = \langle \lambda|\mu\rangle \ . \tag{1}$$

(2) The solution of the Lippmann-Schwinger (LS) equation for the transition operator ($\hat{T}$) relative to the outgoing electron—see, e.g., Ref. 10—in the subspace of the discrete L^2 functions and with the projected potential $\hat{V}^t$:

$$\hat{T}^t = \hat{V}^t + \hat{V}^t \hat{G}_0^- \hat{T}^t \ , \tag{2}$$

where $\hat{G}_0^-$ is the free-particle Green function for the ingoing wave boundary condition.

(3) The construction of the LS wave function for the outgoing electron in terms of $\hat{T}^t$

$$\chi^t_{\mathbf{k}}(\mathbf{r}) = e^{i\mathbf{k}\cdot\mathbf{r}} + \hat{G}_0^- \hat{T}^t e^{i\mathbf{k}\cdot\mathbf{r}} \tag{3}$$

and its matching, in the asymptotic region, with the eigenfunctions, relative to the Auger energy, of the long-range Hamiltonian, where the scattering potential $\hat{V}$ has been replaced by its long-range component $\hat{V}^{\mathrm{LR}}$.

(4) The complete evaluation of the transition matrix elements between the initial (almost bound) state and the various final states of the doubly ionized molecule, where the states are represented by specifically optimized Hartree-Fock wave functions.

We note that as far as the first two points are concerned our approach is analogous to the discrete basis function method for nonspherical potentials introduced by Rescigno, McCurdy, and McKoy[11–13] for treating electron-molecule scattering, while the technique for the evaluation of the Auger matrix element [point (4)] and the bound-free integrals required in it have been developed by the authors in Refs. 5, 14–16.

The outline of this paper is the following. In Sec. II we describe the method. In Sec. III we give the technical procedures for its implementation and consider a specific atomic problem (the *KLL* Auger spectrum of neon) for which accurate numerical results are available. In Sec. IV we apply our method to the evaluation of Auger transition rates in the LiF molecule, improving previous results (see Ref. 5) obtained by the authors on this molecule with a simplified description of the continuum orbital.

II. THE METHOD

Following the approach described in Ref. 5, the computed quantity we compare with the measured Auger rate for each decay channel β is the following:

$$W_\beta = \frac{k}{(2\pi)^2}\int |\langle \Phi|H-E_\Phi|\Psi_{\beta,\mathbf{k}}\rangle|^2 d\hat{\mathbf{k}} , \tag{4}$$

given in a.u., where Φ is a quadratic-integrable normalized wave function for the resonant (almost bound) initial state, whose energy is $E_\Phi = \langle \Phi|H|\Phi\rangle$ and $\Psi_{\beta,\mathbf{k}}$ is a representation of the decay channel β identified asymptotically by the energy E_β of the doubly ionized molecule and by the energy ε_k of the outgoing electron: $\varepsilon_k = E_\Phi - E_\beta = \frac{1}{2}k^2$. Note that in (4) we perform an integration over the directions of the outgoing electron, since the Auger spectra we want to interpret identify each decay channel only in terms of the kinetic energy of the Auger electron.

To represent the initial (almost bound) state and the final states of the doubly ionized molecule we use Hartree-Fock (HF) wave functions, each one obtained with a separate self-consistent field (SCF) process, thus disregarding electronic correlation effects, apart from those due to the antisymmetrization of the wave functions. Each final wave function $\Psi_{\beta,\mathbf{k}}$ is written as an antisymmetrized product of the following type:

$$\Psi_{\beta,\mathbf{k}} = \left[\frac{1}{(N+1)!}\right]^{1/2} \hat{A}[\Theta_\beta(1,2,\ldots,N)\eta_{\beta,\mathbf{k}}(N+1)] , \tag{5}$$

where Θ_β is the HF wave function for the doubly ionized molecule in the state β, $\eta_{\beta,\mathbf{k}}$ is the spin orbital for the outgoing electron given in the form

$$\eta_{\beta,\mathbf{k}}(1) = \chi_{\beta,\mathbf{k}}(\mathbf{r}_1)\sigma_\beta(s_1) , \tag{6}$$

and the normalization of $\Psi_{\beta,\mathbf{k}}$ is chosen to be

$$\langle \Psi_{\beta,\mathbf{k}}|\Psi_{\beta',\mathbf{k}'}\rangle = (2\pi)^3\delta(\mathbf{k}-\mathbf{k}')\delta_{\beta,\beta'} . \tag{7}$$

The use of an independent-particle representation of the states leads to the choice of the continuum orbital $\chi_{\beta,\mathbf{k}}$ as the eigenfunction, relative to the energy ε_k, of the HF Hamiltonian $\hat{F}_\beta$ for $\chi_{\beta,\mathbf{k}}$ in $\Psi_{\beta,\mathbf{k}}$:

$$\hat{F}_\beta(\mathbf{r})\chi_{\beta,\mathbf{k}}(\mathbf{r}) = \varepsilon_k\chi_{\beta,\mathbf{k}}(\mathbf{r}) , \tag{8}$$

where $\hat{F}_\beta$ is defined in terms of the nonlocal static-exchange potential $\hat{V}_\beta$ as follows:

$$\begin{aligned}\hat{F}_\beta(\mathbf{r}) &= -\tfrac{1}{2}\hat{\nabla}_{\mathbf{r}}^2 - \sum_\alpha \frac{Z_\alpha}{|\mathbf{r}-\mathbf{R}_\alpha|} \\ &\quad + \sum_{j=1}^{N}[a_j^{(\beta)}\hat{J}_j^{(\beta)}(\mathbf{r}) - b_j^{(\beta)}\hat{K}_j^{(\beta)}(\mathbf{r})] \\ &= -\tfrac{1}{2}\hat{\nabla}_{\mathbf{r}}^2 + \hat{V}_\beta(\mathbf{r},\{\mathbf{R}\}) .\end{aligned} \tag{9}$$

In (9) Z_α and $\mathbf{R}_\alpha$ are, respectively, the charge and position of the αth nucleus in the molecule, while $\hat{J}_j^{(\beta)}$ and $\hat{K}_j^{(\beta)}$ are the usual Coulomb and exchange operators weighted by coefficients that are related to the occupation number of the jth orbital in Θ_β.

We observe that in the Auger problem $\hat{V}_\beta(\mathbf{r},\{\mathbf{R}\})$ is a long range potential:

$$\hat{V}_\beta(\mathbf{r},\{\mathbf{R}\}) \underset{r\to\infty}{\sim} \hat{V}_\beta^{\mathrm{LR}}(\mathbf{r},\{\mathbf{R}\}) \simeq -\frac{2}{r} + O\left[\frac{1}{r^n}\right] , \tag{10}$$

with a tail represented by a Coulomb potential plus higher-order corrections that depend on the type of molecule considered. (Note that from now on we will call the "asymptotic" region that part of the space in which $\hat{V}_\beta \simeq \hat{V}_\beta^{\mathrm{LR}}$). Because of the presence of a long-range, Coulomb potential to obtain $\chi_{\beta,\mathbf{k}}$ in (8), via the solution of the corresponding Lippmann-Schwinger equation, one should include in the zeroth-order Hamiltonian at least the Coulomb and static dipole components of the potential,[17] but the technical implementation of this requirement would present serious difficulties in a molecular context.

What we suggest, following Rescigno, McCurdy, and McKoy,[11-13] is the approximate representation of $\hat{V}_\beta$ in (9) by means of its expansion ($\hat{V}_\beta^t$) in a finite discrete basis set of L^2 functions—see Eq. (1)—chosen in such a way as to minimize the difference $(\hat{V}_\beta - \hat{V}_\beta^t)|\chi_{\beta,\mathbf{k}}\rangle$ inside the region of interest. The replacement ($\hat{V}_\beta^t \to \hat{V}_\beta$) allows one to solve the LS equation (2) for the transition operator $\hat{T}^t$ at ε_k, since Eq. (2) becomes a matrix equation with solution

$$\underline{T}^t = [\underline{1} - \underline{V}_\beta^t\underline{G}_0^-(\varepsilon_k)]^{-1}\underline{V}_\beta^t . \tag{11}$$

Note that, if $\underline{V}^t$ can be inverted, one can use equivalently the following symmetrized expression for the matrix representation of $\hat{T}$:

$$\underline{T}^t = \underline{V}_\beta^t[\underline{V}_\beta^t - \underline{V}_\beta^t\underline{G}_0^-(\varepsilon_k)\underline{V}_\beta^t]^{-1}\underline{V}_\beta^t . \tag{12}$$

The corresponding LS wave function satisfying the ingoing-wave boundary condition is defined in (3) and represents an eigenvector, relative to the energy ε_k, of $\hat{F}_\beta^t$, i.e., of an effective Hamiltonian defined as in (9), but with $\hat{V}_\beta$ replaced by $\hat{V}_\beta^t$, i.e., by its basis set representation defined as in (1). Using Eqs. (1), (3), and (12) one can write $\chi_{\beta,\mathbf{k}}^t$ in the form:

$$\chi_{\beta,\mathbf{k}}^t = e^{i\mathbf{k}\cdot\mathbf{r}} + \sum_\lambda c_\lambda(\mathbf{k},\varepsilon_k)f_\lambda(\varepsilon_k,\mathbf{r}) , \tag{13}$$

with

$$\begin{aligned} c_\lambda &= \sum_{\mu,\nu,\tau} S_{\lambda\mu}^{-1}\langle\mu|\hat{T}^t(\varepsilon_k)|\nu\rangle S_{\nu\tau}^{-1}\langle\tau|\mathbf{k}\rangle , \\ S_{\lambda\mu} &= \langle\lambda|\mu\rangle \end{aligned} \tag{14}$$

$$f_\lambda(\varepsilon_k,\mathbf{r}) = \hat{G}_0^-(\varepsilon_k)|\lambda\rangle . \tag{15}$$

The general expressions of the continuum functions $\{f_\lambda\}$, obtained by applying the free-particle Green function to Hermite Gaussian Functions (HGF) of any order and center, together with the expressions of their derivatives with respect to $\mathbf{r}$, have been derived by the authors in Ref. 16; both these quantities are necessary for matching $\chi_{\beta,\mathbf{k}}^t$ with the eigenfunctions of the long-range Hamiltonian $\hat{F}_\beta^{\mathrm{LR}}$, where $\hat{V}_\beta$ has been replaced by $\hat{V}_\beta^{\mathrm{LR}}$—see Sec. III.

In regards to the Auger matrix element, instead, only the L^2 components of $\chi_{\beta,\mathbf{k}}^t$ are important, since both the initial (Φ) and the final (Θ_β) states are given in terms of

bound orbitals, and, in fact, the difference between the values obtained using the LS wave function as given in (13), or its projection onto an adequate basis set of the HFG are smaller than a few parts in 10^4, as shown by our test calculations.

The crucial point in this type of approach is the replacement ($\hat{V}_\beta^t \rightarrow \hat{V}_\beta$), which seems particularly delicate, involving as it does truncation of the long-range part of the HF potential, although it is clear that the Auger matrix element is really sensitive to the form of the continuum orbital only inside the molecular region.

The way we suggest to properly perform such a replacement is based on the idea that it should be sufficient to have a projected potential $\hat{V}_\beta^t$, which, applied to $\chi_{\beta,\mathbf{k}}^t$ correctly reproduces the effect of the true potential $\hat{V}_\beta$ on $\chi_{\beta,\mathbf{k}}^t$ continuing into at least a part of the asymptotic region. (Note that from now on we will call the "intermediate asymptotic" region that part of the asymptotic region for which $[\hat{V}_\beta^{\mathrm{LR}} - (\hat{V}_\beta^{\mathrm{LR}})^t]|\chi_{\beta,\mathbf{k}}^t\rangle \simeq 0$, where $(\hat{V}_\beta^{\mathrm{LR}})^t$ is the basis set representation of $\hat{V}_\beta^{\mathrm{LR}}$). In that case the LS wave function within this intermediate asymptotic region will be a linear combination of the eigenfunctions of $\hat{F}_\beta^{\mathrm{LR}}$ corresponding to the Auger energy. These eigenfunctions, for the usual problems, are known analytically or in any case can be easily obtained by using standard numerical techniques and therefore it should be possible to set up a procedure for matching them to the LS wave function in order to obtain the correct asymptotic behavior.

The implementation of such an idea requires establishing a criterion for the choice of a basis set able to represent the scattering potential and defining procedures to connect the LS wave function with the analytical or numerical eigenfunction of $\hat{F}_\beta^{\mathrm{LR}}$ relative to the Auger energy. These two problems will be extensively studied in Sec. III.

III. TECHNICAL PROCEDURES

In the first part of this section we propose a criterion for the choice of the discrete basis set to be used for representing the HF potential as shown in (1). Then, in the second part, we apply this technique to a specific atomic problem (the *KLL* Auger spectrum of the atomic neon), discuss the technical procedures for matching the LS wave function with the eigenfunctions of $\hat{F}_\beta^{\mathrm{LR}}$ relative to the Auger energy of interest, and finally suggest a simplified approach useful for molecular problems.

A. Choice of the basis set

As in Ref. 18, we distinguish between two discrete basis sets of Hermite Gaussian functions: a smaller one, that used for the standard SCF calculations for the bound orbitals of the initial and final states, and a larger basis set that includes the previous one plus other functions, that constitute the so-called scattering basis set, which is used for computing the matrix elements of the static-exchange potential. The extension of the SCF basis set, realized by adding diffuse functions, but also making more dense the basis set in certain regions of the non-linear parameters, is necessary to obtain for the potential a correct reproduction extending as far as the intermediate asymptotic region.

If one can assume negligible the difference $(\hat{V}_\beta - \hat{V}_\beta^t)|\chi_{\beta,\mathbf{k}}^t\rangle$ as far as this region, the matching of $\chi_{\beta,\mathbf{k}}^t$ with the eigenfunctions of $\hat{F}_\beta^{\mathrm{LR}}$, relative to the Auger energy, will be smooth and practically independent on the position of the matching point, provided that this be internal to the intermediate asymptotic region. From the requirement of continuity of $\chi_{\beta,\mathbf{k}}^t$ and of its first derivative at the matching point one can obtain the matching parameters, whose stability with respect to changes in the position of the matching point will be a stringent test of the quality of the chosen basis set. Satisfaction of this requirement of stability is the first criterion we propose for the choice of the basis functions.

The second one involves the variational stability of the Auger decay rate W_β with respect to changes in the basis set: this requirement is introduced in order to reduce the fluctuations of the computed quantities due to changes in the quality of the representation of $\hat{V}_\beta$. In practice, what we are looking for is a criterion for setting up a scattering basis set in such a way as to obtain simultaneously an extremal point of W_β with respect to the parameters that characterize this basis set, together with a stable matching between $\chi_{\beta,\mathbf{k}}^t$ and the eigenfunctions of $\hat{F}_\beta^{\mathrm{LR}}$ relative to the Auger energy.

To this end we employ a procedure suggested by the analysis of the variational stability of the scattering amplitude proposed by McKoy *et al.* in Refs. 18 and 19. Following the Kohn's prescription[20] they show that one can variationally correct the K-matrix elements, obtained via the LS equation, by adding to them the following term: $\langle \chi_{\beta,\mathbf{k}'}^{(-)}|\hat{F}_\beta - \varepsilon_k|\chi_{\beta,\mathbf{k}}^{(+)}\rangle$. Furthermore, they argue that this matrix element vanishes through first order in $\hat{V}_\beta - \hat{V}_\beta^t$ at the eigenenergies of the projected $\hat{F}_\beta$, at least for low-scattering energy, i.e., when the LS wave function is dominated by the lowest contributing partial wave and therefore can be assumed proportional to the corresponding eigenfunction of the projected $\hat{F}_\beta$.

In our problem the quantity to be considered is the Auger matrix element in W_β, to which only those (lm) components of the LS wave function contribute that are selected by the symmetry of the initial (Φ) and final (Θ_β) states, and therefore the assumption of the proportionality of these components to the corresponding eigenfunctions of the projected Hamiltonian does not depend on approximation of the boundary conditions for nonspherical potential.[19] Therefore it seems reasonable to look for a representation of $\hat{V}_\beta$ in terms of a discrete basis set that includes eigenvectors of the projected $\hat{F}_\beta$ relative to the Auger energy of interest, such eigenvectors being the most important in an L^2 representation of the continuum orbital.

The technical procedure for implementing this idea will be described in Sec. III B for the specific case of the *KLL* Auger spectrum of the atomic neon, but here we want to point out the main conclusions that can be drawn from our experience. They can be summarized as follows.

(1) Identifying each scattering basis set of symmetry functions by means of a single parameter, viz., a scale factor (q), that multiplies all the orbital exponents of the basis functions, it has been found that each Auger decay rate W_β, considered as a function of q, reaches a minimum for a value ($\bar{q}$) very close to that for which the discrete basis set includes an eigenvector of the projected $\hat{F}_\beta$ relative to the Auger energy of interest.

(2) By increasing progressively the number of basis functions it is possible to find a $\bar{q}$ for which also the matching between the LS wave function and the eigenfunctions of $\hat{F}_\beta^{\mathrm{LR}}$, relative to the Auger energy of interest, is smooth and stable.

(3) For this scattering basis set, changing progressively the value of q away from $\bar{q}$ causes W_β to increase up to a maximum and then decrease again. Taking the geometrical average between the values of two neighboring minimum and maximum one gets a quite good estimate (relative errors less than 7% in our test calculations) of the "exact" value of W_β, i.e., of the value obtained by using the LS wave function smoothly joined with the eigenfunctions of $\hat{F}_\beta^{\mathrm{LR}}$ relative to the Auger energy of interest.

B. An atomic example: the *KLL* Auger spectrum of the neon

It is clear that in the atomic case only one (lm) component of the LS wave function (13) contributes to a given W_β, precisely that determined by the symmetry of the initial (almost bound) state Φ and of the final state Θ_β of the doubly ionized atom—see Eqs. (4) and (5). Furthermore since we use HF potentials which are spherically symmetrized, the only long-range component to be considered is the Coulomb one, and the matching conditions at a given r_0, internal to the intermediate asymptotic region, can be chosen as follows for any given (lm) component of $\chi^t_{\beta,\mathbf{k}}$:

$$
\begin{aligned}
&[\langle Y_{lm}(\hat{\mathbf{r}})|\chi^t_{\beta,\mathbf{k}}(\mathbf{r})\rangle]_{r=r_0} \\
&\quad = 4\pi i^l j_l(kr_0) Y^*_{lm}(\hat{\mathbf{k}}) \\
&\qquad + \sum_\lambda c_\lambda(\varepsilon_k,\mathbf{k})[\langle Y_{lm}(\hat{\mathbf{r}})|f_\lambda(\varepsilon_k,\mathbf{r})\rangle]_{r=r_0} \\
&\quad = N_l(\varepsilon_k) 4\pi Y^*_{lm}(\hat{\mathbf{k}}) C_l(\varepsilon_k,r_0)\ , \qquad (16)
\end{aligned}
$$

$$
\left[\frac{d}{dr}\langle Y_{lm}(\hat{\mathbf{r}})|\chi^t_{\beta,\mathbf{k}}(\mathbf{r})\rangle\right]_{r=r_0}
= N_l(\varepsilon_k) 4\pi Y^*_{lm}(\hat{\mathbf{k}}) \left[\frac{dC_l(\varepsilon_k,r)}{dr}\right]_{r=r_0}\ . \qquad (17)
$$

In (16) $j_l(kr_0)$ is a spherical Bessel function, $C_l(\varepsilon_k,r_0)$ a shifted Coulomb function, whose asymptotic behavior gives the phase shift δ_l with respect to a regular Coulomb function, and $N_l(\varepsilon_k)$ a matching parameter that goes to 1 when $\hat{V}^t_\beta$ goes to 0. The fact that $N_l(\varepsilon_k)$ will be in general different from 1 is essentially due to the different asymptotic behavior of $\hat{V}^t_\beta$ as compared to that of the true potential $\hat{V}_\beta$, a difference that remains also if $(\hat{V}_\beta - \hat{V}^t_\beta)|\chi^t_{\beta,\mathbf{k}}\rangle$ is negligible as far as the intermediate asymptotic region.

The technical procedures for computing N_l, δ_l, and W_β can be summarized as follows.

1. Determination of the radius (r_0) of the short-range component of $\hat{V}_\beta$

This can be easily performed, for example, by plotting the local part of $\hat{V}_\beta$ as function of r in comparison with its long-range component: $\hat{V}_\beta^{\mathrm{LR}} = -2/r$. In Fig. 1 we make this comparison in the case of the $^1D(2p^{-1}2p^{-1})$ state for which the symmetrized HF potential is given by

$$
\begin{aligned}
\hat{V}_\beta(\mathbf{r}) = &-\frac{10}{|\mathbf{r}|} + \sum_s [2J_s(\mathbf{r}) - K_s(\mathbf{r})] \\
&+ \tfrac{2}{3}\sum_t [2J_t(\mathbf{r}) - K_t(\mathbf{r})] \\
&(\phi_s = 1s, 2s)\ \ (\phi_t = 2p_x, 2p_y, 2p_z)\ . \qquad (18)
\end{aligned}
$$

From this figure one can see that the short-range component ($\hat{V}_\beta - \hat{V}_\beta^{\mathrm{LR}}$) of the HF potential is practically exhausted at $r \sim 1.9$ a.u., a value that has been obtained also for the other states.

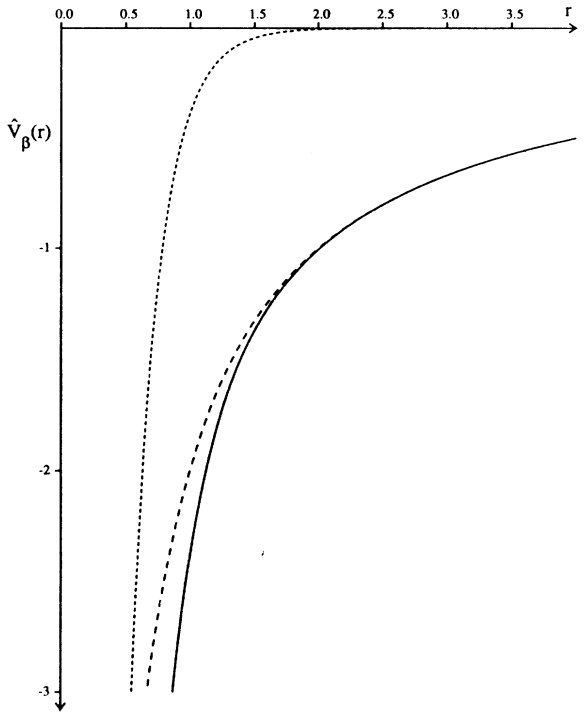

FIG. 1. Dependence on r of the Hartree-Fock potential $\hat{V}_\beta$ defined in (18) (——) and of its long-range (— — —) and short-range (----) components. All the quantities are given in atomic units.

2. *Construction of the LS wave function*

To this end we have used Eq. (3) with $\hat{V}_\beta$ represented in a basis set, which contains an eigenvector of the projected $\hat{F}_\beta$ at the Auger energy of interest to guarantee the variational stability of W_β with respect to changes in the basis set. In Fig. 2 for the state ^1D we show the behavior with r of the real part of the radial function $g_{2,-2}(r)$, obtained by extracting the $(2,-2)$ component of $\chi^t_{\beta,\mathbf{k}}$ as follows:

$$\frac{4\pi}{r} Y^*_{2,-2}(\hat{\mathbf{k}}) g_{2,-2}(r) = \frac{4\pi}{r} Y^*_{2,-2}(\hat{\mathbf{k}})[g^{(\mathrm{PW})}_{2,-2}(r) + g^{(\mathrm{LS})}_{2,-2}(r)]$$
$$= \langle Y_{2,-2}(\hat{\mathbf{r}}) | e^{i\mathbf{k}\cdot\mathbf{r}} \rangle + \langle Y_{2,-2}(\hat{\mathbf{r}}) | \hat{G}_0^- \hat{T}^t e^{i\mathbf{k}\cdot\mathbf{r}} \rangle \ . \quad (19)$$

In Fig. 2 we also compare separately the behavior of its plane-wave part $g^{(\mathrm{PW})}_{2,-2}$ and LS correction $g^{(\mathrm{LS})}_{2,-2}$ showing that the LS correction stabilizes as a periodic function at about $r \sim 3$ a.u. (a distance at which $\hat{V}^t_\beta$ is practically exhausted) and largely reduces the amplitude of the total wave, being shifted with respect to the plane-wave component. In regards to the imaginary part of $g_{2,-2}$ we observe that only the LS correction contributes to it, giving a function that is obviously proportional to the real part of $g_{2,-2}$ since both are solutions of the same equation for the same energy and boundary conditions. Furthermore, to give an idea of the degree of accuracy that can be obtained by using expansions in terms of HGF, we compare in Fig. 3, for the state ^1D, the dependence on r of $\hat{V}^t_\beta$ with those of $\hat{V}^{\mathrm{LR}}_\beta$ and of its basis set representation $(\hat{V}^{\mathrm{LR}}_\beta)^t$ when applied to the real part of the radial function

TABLE I. Modulus of the expansion coefficients (a_j) of the $(2,-2)$ component of the LS wave function, relative to the $^1D(2p^{-1}2p^{-1})$ state and to the $(\vartheta_k=\pi/2, \varphi_k=\pi/4)$ direction, on the basis of the eigenvectors of the projected $\hat{F}_\beta$. The ε_j are the corresponding eigenvalues and the Auger energy (ε_k) is equal to 29.621 181 a.u. All the quantities are given in atomic units.

a_j	ε_j
0.000 062	−0.225 681
0.000 363	−0.097 512
0.000 742	0.082 740
0.001 201	0.371 222
0.001 829	0.807 400
0.002 691	1.454 452
0.003 885	2.409 052
0.005 440	3.814 942
0.007 410	5.883 554
0.009 611	8.924 148
0.011 961	13.392 591
0.013 749	19.957 937
0.637 097	29.621 152[a]
0.016 688	43.855 811
0.016 062	64.945 648
0.015 609	96.263 044
0.013 924	143.584 677
0.012 738	215.439 157
0.010 430	331.652 243
0.009 390	522.966 634

[a]This value corresponds most closely to the Auger energy.

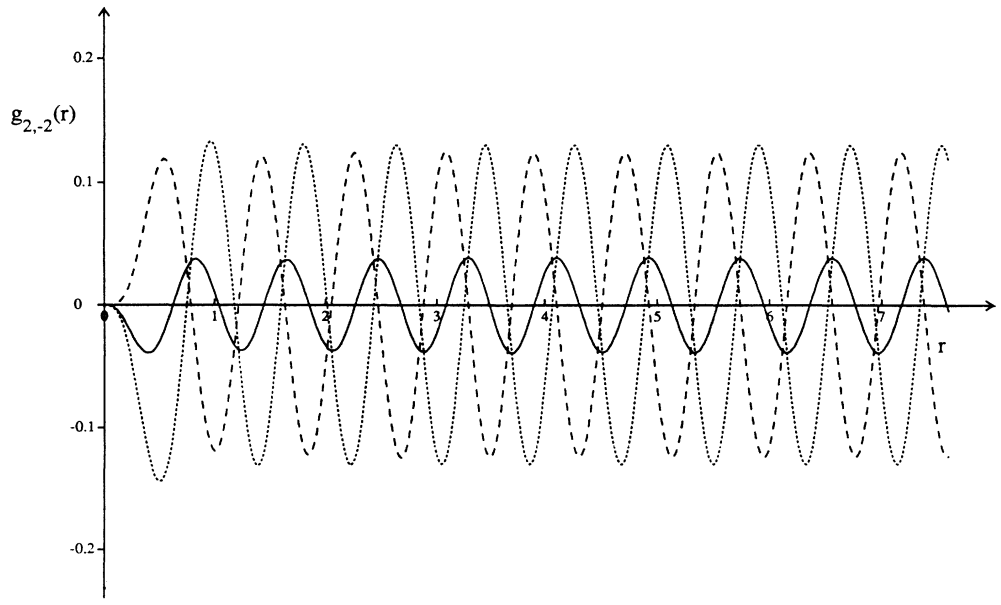

FIG. 2. Dependence on r of the real part of the radial function $g_{2,-2}(r)$ (——) of its plane-wave component $g^{(\mathrm{PW})}_{2,-2}(r)$ (- - - -) and LS correction $g^{(\mathrm{LS})}_{2,-2}(r)$ (— — —) for the state ^1D. The direction chosen for $\hat{\mathbf{k}}$ is $(\theta_k=\pi/2, \phi_k=\pi/4)$. All the quantities are given in atomic units.

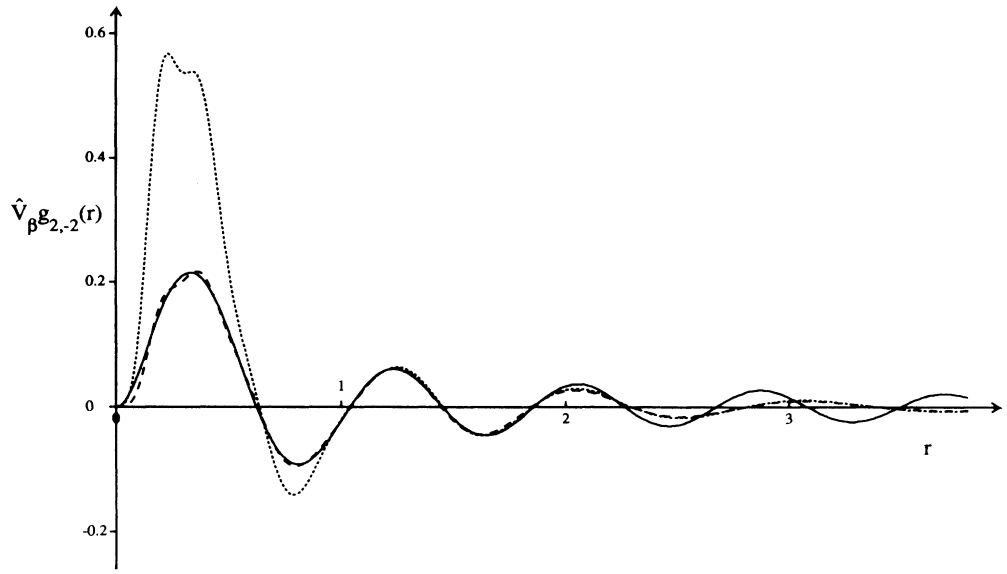

FIG. 3. Dependence on r of the real part of $\hat{V}_\beta^t g_{2,-2}(r)$ (----), $(\hat{V}_\beta^{\mathrm{LR}})^t g_{2,-2}(r)$ (— — —), and $\hat{V}_\beta^{\mathrm{LR}} g_{2,-2}(r)$ (——) for the state ^1D. The direction chosen for $\hat{\mathbf{k}}$ is $(\theta_k=\pi/2,\phi_k=\pi/4)$. All the quantities are given in atomic units.

$g_{2,-2}(r)$. From this figure one can see that in the region between $r\sim 1$ a.u. and $r\sim 2.3$ a.u., one has

$$\hat{V}_\beta^t g_{2,-2}(r)\simeq(\hat{V}_\beta^{\mathrm{LR}})^t g_{2,-2}(r)\simeq\hat{V}_\beta^{\mathrm{LR}} g_{2,-2}(r)$$

and this fact confirms the high degree of accuracy obtained by our basis set representation as far as these distances. Note that in the inner region ($r<1$ a.u.) the short-range components of $\hat{V}_\beta$ are dominant and therefore $\hat{V}_\beta$ is very different from $\hat{V}_\beta^{\mathrm{LR}}$; that, however, is very well represented by $(\hat{V}_\beta^{\mathrm{LR}})^t$, while for $r>2.3$ a.u. the reproduction of $\hat{V}_\beta^{\mathrm{LR}}$ in terms of HGF becomes unavoidably very poor. Finally in Table I we give the expansion coefficients of the LS wave function for the state ^1D on the basis of the eigenvectors of the projected $\hat{F}_\beta$, in order to show that the eigenvector at the Auger energy contributes to this expansion at least 40 times more than any other eigenfunction. This fact, on the one hand confirms the validity of the assumption of proportionality between the LS component of interest and the eigenvector relative to the Auger energy, and on the other hand, together with the variational stability of W_β discussed at the end of this section, gives a further justification to our criterion for the choice of the basis set.

3. *Matching between the LS wave function and $C_l(\varepsilon_k,r)$*

This is performed as shown in Eqs. (16) and (17) by constructing $C_l(\varepsilon_k,r)$ via the solution of the radial equation for $\hat{V}_\beta^{\mathrm{LR}}$ from r_0 to "infinity"—through, for example, the Runge-Kutta method[21]—and using as input data the value of the radial function $\langle Y_{lm}(\hat{\mathbf{r}})|\chi_{\beta,\mathbf{k}}^t\rangle$ and of its first derivative at r_0 (for the details of the matching procedure see Ref. 16). In Table II we give, for all the states of interest, the values of the matching parameters N_l and δ_l, calculated at various r_0 in the intermediate asymptotic region, together with a few data defining the scattering basis sets. The stability of these parameters with respect to the position of the matching point represents a proof of the proper quality of the basis sets used. We observe that the value of the scale factor N_l is practically the same for all the states, while the phase shift δ_l is mainly a function of l going approximately at $\delta_l\sim\tilde{\delta}(l,s)/(l+1)$ where $\tilde{\delta}(l,s)$ is a smooth function of l and of the spin number s.

4. *Evaluation of the Auger decay rate W_β*

Applying our method to an atomic case, where only one (lm) component of the continuum orbital contributes to the Auger matrix element, the radial part of this component is given by

$$\frac{4\pi}{r}Y_{lm}^*(\hat{\mathbf{k}})g_{lm}(r)=\begin{cases}\dfrac{1}{N_l}\langle Y_{lm}(\hat{\mathbf{r}})|\chi_{\beta,\mathbf{k}}^t\rangle, & r\le r_0 \quad (20a)\\ 4\pi Y_{lm}^*(\hat{\mathbf{k}})C_l(\varepsilon_k,r), & r\ge r_0 \quad (20b)\end{cases}$$

where $g_{lm}(r)$ is defined by analogy with $g_{2,-2}(r)$ in (19). This means that the continuum orbital to be used coincides with the (lm) component of the LS wave function, scaled according to Eqs. (16) and (17), as far as to the intermediate asymptotic region and then with its analytic continuation in terms of a shifted Coulomb function. However, since the Auger matrix element in (4) is practically insensitive to the asymptotic behavior of the continuum orbital, in the calculation of W_β we have used only its LS part properly scaled as shown in (20a), thus avoiding the problem of the integration over finite volumes. Note that in the calculation of W_β one has to take into account also the fact that the bound orbitals of the initial and final states are mutually nonorthogonal since they

TABLE II. Values of the matching parameters: N_l and δ_l, calculated at various matching points r_0, for all the Auger states of interest. In column 2 we report the number and type of functions and the maximum (α_{max}) and minimum (α_{min}) values of the orbital exponents of the scattering basis functions used to calculate the Auger decay rates. All the quantities are given in atomic units.

State	Scattering basis set: Number and type of function	Scattering basis set: α values of orbital exponents	r_0	N_l	δ_l
$^1S(2s^{-1}2s^{-1})$	15 s	$\alpha_{max}=82.1943$	1.90	0.965	1.821
		$\alpha_{min}=0.0071$	1.92	0.965	1.820
			1.94	0.966	1.819
			1.96	0.966	1.817
			1.98	0.965	1.816
			2.00	0.965	1.815
$^1P(2s^{-1}2p^{-1})$	15 p	$\alpha_{max}=44.7795$	1.90	0.960	1.009
		$\alpha_{min}=0.0086$	1.92	0.959	1.009
			1.94	0.959	1.008
			1.96	0.959	1.008
			1.98	0.959	1.008
			2.00	0.959	1.008
$^3P(2s^{-1}2p^{-1})$	15 p	$\alpha_{max}=139.3347$	1.90	0.963	0.954
		$\alpha_{min}=0.0063$	1.92	0.963	0.953
			1.94	0.962	0.952
			1.96	0.962	0.952
			1.98	0.963	0.953
			2.00	0.964	0.953
$^1S(2p^{-1}2p^{-1})$	15 s	$\alpha_{max}=58.6488$	1.90	0.963	1.783
		$\alpha_{min}=0.0037$	1.92	0.963	1.781
			1.94	0.962	1.780
			1.96	0.962	1.779
			1.98	0.962	1.778
			2.00	0.962	1.778
$^1D(2p^{-1}2p^{-1})$	20 d	$\alpha_{max}=56.9479$	1.90	0.967	0.569
		$\alpha_{min}=0.0494$	1.92	0.967	0.569
			1.94	0.967	0.569
			1.96	0.967	0.568
			1.98	0.968	0.568
			2.00	0.968	0.567

derive from different SCF processes, and that, because of the antisymmetrization of $\Psi_{\beta,\mathbf{k}}$ in (5), it is not necessary to introduce explicitly the orthogonalization of $\chi^t_{\beta,\mathbf{k}}$ to the bound orbitals of Θ_β.

Finally in Tables III and IV we summarize our results, respectively, for the Auger energies and the partial and total Auger rates of various decay channels from Ne[$^2S(1s^{-1})$] and compare them with the results obtained by Kelly in Ref. 22 using a numerical technique and also with the experimental values reported in Refs. 23 and 24. Note that for the bound-state calculations we have used an SCF basis set taken from Ref. 25.

With regards to the HF energies we observe that our results, which are practically coincident with those of Kelly, allow a very accurate estimate of the experimental transition energies (the largest difference is less than 0.3%). This fact is essentially due to the cancellation of the correlation errors between the initial and final states.

TABLE III. Hartree-Fock energies (E_{HF}) and energy differences with respect to the initial state of Ne[$^2S(1s^{-1})$], calculated by us (ΔE_{HF}), by Kelly (ΔE^K_{HF}) (Ref. 22) and compared with the experimental values (Ref. 22). The energies are given in atomic units, while the energy differences are in eV.

State	E_{HF}	ΔE_{HF}	ΔE^K_{HF}	ΔE_{expt}
$^2S(1s^{-1})$	−96.625 752			
$^1S(2s^{-1}2s^{-1})$	−124.076 682	746.97	746.99	748.0±0.1
$^1P(2s^{-1}2p^{-1})$	−124.954 194	770.85	770.86	771.4±0.1
$^3P(2s^{-1}2p^{-1})$	−125.400 826	783.00	783.01	782.0±0.1
$^1S(2p^{-1}2p^{-1})$	−126.060 552	800.95	800.97	800.4±0.1
$^1D(2p^{-1}2p^{-1})$	−126.246 933	806.02	806.04	804.2±0.4

TABLE IV. Partial and total Auger rates for the decay process from Ne[$^2S(1s^{-1})$], calculated using our method (W), using our simplified approach ($\tilde{W}$) described in Sec. III and calculated by Kelly (W_K). In the last column we report the experimental values measured by Koerber and Mehlhorn (W_{KM}) (Ref. 23) and also the total Auger rates measured, respectively, by Gelius *et al.* (W_G^{tot}) (Ref. 24) and Koerber and Mehlhorn (W_{KM}^{tot}). All the quantities are given in 10^{-3} a.u.

State	W	$\tilde{W}$	W_K	W_{KM}
$^1S(2s^{-1}2s^{-1})$	1.0017	1.0131	0.9508	0.35±0.07
$^1P(2s^{-1}2p^{-1})$	2.1765	2.2038	2.0335	0.96±0.19
$^3P(2s^{-1}2p^{-1})$	0.7845	0.8289	0.7888	0.35±0.07
$^1S(2p^{-1}2p^{-1})$	0.4427	0.4749	0.4560	0.55±0.11
$^1D(2p^{-1}2p^{-1})$	5.6408	5.6909	5.6849	3.28±0.066
Total	10.0462	10.2116	9.9140	$W_{KM}^{tot}=5.49\pm0.51$ $W_G^{tot}=8.452\pm0.73$

With regards to the Auger decay rates instead, we want to point out that our method, based on expansions of the potential and the orbitals in terms of finite basis sets, is able to reproduce, within an accuracy of about 7%, the Auger rates calculated by Kelly using a numerical procedure, the residual discrepancies being attributable to the fact that Kelly approximates the transition matrix elements by means of the Wentzel formula instead of using the complete expression given in (4) with different orbitals for the different final states.

Finally, we observe that our Auger decay rates, calculated in the limit of an independent-particle approximation for the various states, differ appreciably from the experimental values, even if a comparison made between the total Auger rate calculated by us and that measured by Gelius *et al.*—see Ref. 24—reduces this difference to about 19%. It is clear that to have a better agreement with the experimental data the inclusion of the correlation effects is essential.

However, since by remaining inside an independent-particle description of the states one cannot hope to reproduce the experimental data beyond a certain limit and, on the other hand, going to molecular problems, other effects—like those related to the coupling between electronic and nuclear motion—become relevant, it can be interesting to look for a simplification of the technique that allows an easier but still sufficiently accurate ($\Delta < 10\%$) estimate of the Auger decay rates obtainable from the full exploitation of our method. Therefore in this paper instead of giving the details of the technical procedures necessary to apply our method to molecular problems, where more than one partial wave in the expansion of $\chi'_{\beta,k}$ contributes to W_β, we show how results, comparable with those previously obtained, can be derived simply by looking at the behavior of W_β as a function of the scale parameter q. From this analysis we will derive a simple way for estimating W_β, that will be used in Sec. IV for predicting the Auger spectrum of the LiF molecule.

Let us consider now the behavior of the Auger decay rate W_β when the scattering basis set is changed by scaling the orbital exponents of the scattering basis functions of a given symmetry. The effect of this change is to shift the eigenvalues of the projected $\hat{F}_\beta$ in such a way that one can finally obtain one eigenvector at the Auger energy of interest (obviously the more reasonable way of doing this is to change q until the closest eigenvalue reaches the Auger energy).

In Fig. 4 we show, for all the states of interest, the behavior of W_β as a function of the distance from the

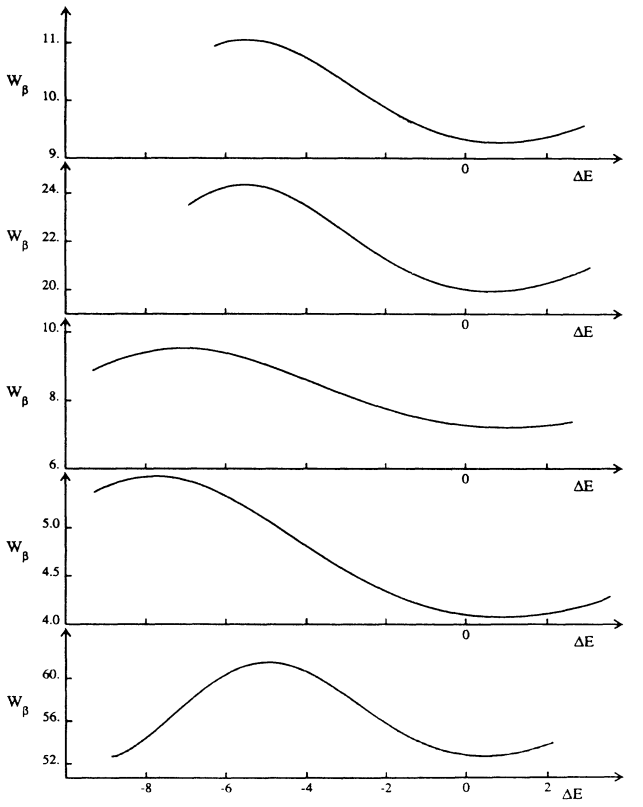

FIG. 4. Behavior of W_β as a function of the difference (ΔE) between the corresponding Auger energy and the eigenvalue of the projected Hamiltonian closest in energy for all the states of interest. The sequence of states is the same one used in Tables II–IV, W_β is given in 10^{-4} atomic units, and ΔE in atomic units.

Auger energy of the closest eigenvalue of the projected Hamiltonian, it being clear that such a distance is a simple function of the scale factor q.

The main conclusions that one can draw from these plots are the following.

(a) W_β is variationally stable when the Auger energy is very close to an eigenenergy of the projected $\hat{F}_\beta$. We observe that the minimum of these curves does not coincide exactly with the Auger energy, but is shifted a little bit toward higher energies. However, such curves are so flat near the minimum that the difference between the value of W_β at the minimum and that at the Auger energy is of a few parts in 10^3.

(b) A sufficiently accurate estimate of W_β can be simply obtained by taking the geometrical average between two adjacent minima and maxima of W_β, whose distance from this average values is at most of the order of 15%.

Note that in Fig. 4 we have shown the presence of a maximum at energies smaller than the Auger one, where usually the density of eigenstates of the projected Hamiltonian is higher, but another maximum, practically of the same magnitude as the previous one, is present also at energies greater than the Auger one. The fact that these two maxima of W_β are very similar in magnitude eliminates every ambiguity in the averaging process.

The results obtained using our simplified approach are summarized in the third column of Table IV and compare very well with our previous ones, the largest difference being of the order of 7%.

Because of the very satisfactory performance of this simplified approach, we have applied it also to the prediction of the Auger spectrum of the LiF molecule, establishing also in this case a confirmation of the variational stability of W_β when there are eigenvectors of the projected $\hat{F}_\beta$ whose eigenvalues are close to the Auger energy and obtaining in this way a very satisfactory reproduction of the experimental spectrum.

IV. CALCULATION OF AUGER DECAY RATES FOR THE LiF MOLECULE

We have applied our method to the calculation of the Auger transition rates of the LiF molecule ionized in its deepest shell, with a view to comparing the results obtained through this new approach with the recent calculations performed by the authors[5] on the same molecule, using a simplified description of the continuum orbital as an orthogonalized plane wave. Moreover, for such a molecule sufficiently accurate measurements of the Auger spectrum of gaseous LiF are available in the range of energy from 600 to 680 eV.[26]

In particular, while for six of the 11 transitions taken into account by the authors in Ref. 5 a satisfactory agreement between calculated and experimental values of the decay rates has been obtained (maximum relative error $\sim 37\%$), for the remaining five transitions the predicted values differ from the experimental ones by a factor ranging between 3 and 7. These discrepancies have been attributed by the authors mainly to an insufficient description of the continuum orbital inside the molecular region, where only the orthogonalization procedure takes into account—and only partially—the presence of the other electrons. Therefore it is quite interesting to see how effective the LS approach is for constructing a continuum orbital, leading to better predictions of the experimental Auger rates.

TABLE V. Number, type, and center of the basis functions of the two scattering basis sets (SBS's) used for each decay state of the LiF molecule, classified according to the hole configuration.

State		SBS No. 1	SBS No. 2
$\pi_+\pi_-$	$^1\Sigma^+$	$6d_F+4d_{Li}$	$(6d_F+4d_{Li})+(3p_F+2p_{Li})$
$4\sigma 4\sigma$	$^1\Sigma^+$	$6d_F+4d_{Li}$	$(6d_F+4d_{Li})+(3p_F+2p_{Li})$
$3\sigma 4\sigma$	$^3\Sigma^+$	$6s_F+4s_{Li}$	$(6s_F+4s_{Li})+(3p_F+2p_{Li})$
$3\sigma 4\sigma$	$^1\Sigma^+$	$6s_F+4s_{Li}$	$(6s_F+4s_{Li})+(3p_F+2p_{Li})$
$3\sigma 3\sigma$	$^1\Sigma^+$	$6s_F+4s_{Li}$	$(6s_F+4s_{Li})+(3p_F+2p_{Li})$
$4\sigma\pi_+$	$^3\Pi$	$6p_F+4p_{Li}$	$(6p_F+4p_{Li})+(3d_F+2d_{Li})$
$4\sigma\pi_+$	$^1\Pi$	$6d_F+4d_{Li}$	$9d_F+6d_{Li}$
$3\sigma\pi_+$	$^3\Pi$	$6p_F+4p_{Li}$	$(6p_F+4p_{Li})+(3d_F+2d_{Li})$
$3\sigma\pi_+$	$^1\Pi$	$6p_F+4p_{Li}$	$(6p_F+4p_{Li})+(3d_F+2d_{Li})$
$\pi_+\pi_+$	$^1\Delta$	$6d_F+4d_{Li}$	$9d_F+6d_{Li}$

To this end we have applied the present method in the simplified form described at the end of Sec. III B, using for the bound orbitals the SCF basis set given in Ref. 5 and calculating the transition rates by means of the geometrical average between two adjacent minima and

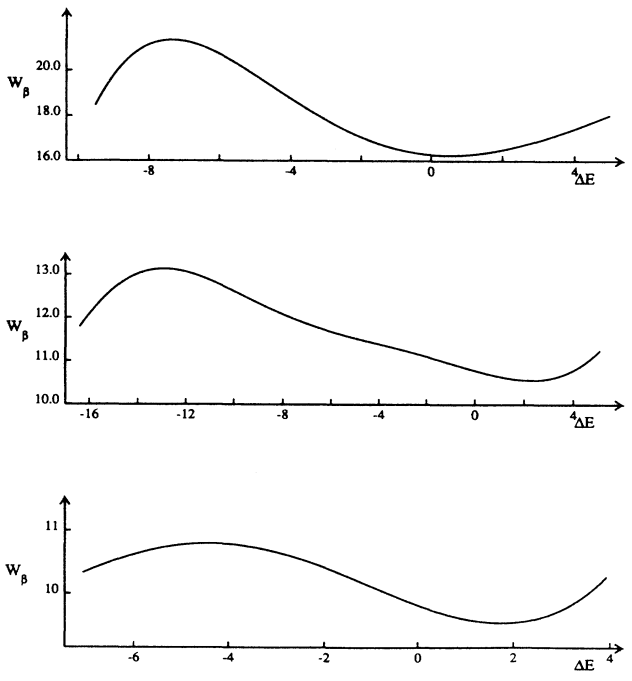

FIG. 5. Behavior of W_β as a function of the difference (ΔE) between the corresponding Auger energy and the eigenvalue of the projected Hamiltonian closest in energy for the following states of the LiF molecule: $^1\Sigma(3\sigma^{-1}3\sigma^{-1})$, $^1\Pi(3\sigma^{-1}\pi_+^{-1})$, $^1\Delta(\pi_+^{-1}\pi_-^{-1})$. W_β is given in 10^{-4} atomic units and ΔE in atomic units.

maxima of W_β considered as a function of the distance between the Auger energy of interest and the closest eigenvalue of the projected Hamiltonian.

We observe that because of the reduced symmetry of the molecule an infinite number of (lm) components of $\chi_{\beta,\mathbf{k}}$ contribute to the Auger matrix element in W_β, and therefore one should include various different types of basis functions in the expansion of the scattering potential. In order to check the stability of our results with respect to the inclusion of different types of scattering functions centered on different positions, we have performed our calculations with two basis sets for each state, chosen in a way appropriate to the nature of the continuum orbital, as summarized in Table V. Furthermore, to simplify our procedure we have used only one scale factor (q) for each scattering basis set, with no distinction as to type of basis function, and this fact produces a shift of the position of the minimum of W_β from the corresponding Auger energy which is larger than in the atomic case because of the presence of different contributions from the different basis set components.

To check this point we present in Fig. 5 the behavior of W_β as a function of the difference between the Auger energy and the closest eigenvalue of the projected Hamiltonian for the three states $^1\Sigma(3\sigma^{-1}3\sigma^{-1})$, $^1\Pi(3\sigma^{-1}1\pi^{-1})$, and $^1\Delta(1\pi^{-1}1\pi^{-1})$. Furthermore we give in Table VI the expansion coefficients of the corresponding LS orbitals with respect to the basis sets of the eigenvectors of the projected $\hat{F}_\beta$ in order to evaluate the relative importance of these orbitals in the description of $\chi^l_{\beta,\mathbf{k}}$.

Figure 5 shows that as in the atomic case the W_β's have an oscillatory behavior and the largest difference between a maximum (minimum) of W_β and the average value is of the order of 15%; the main difference with respect to the atomic case is that in this case the minima suffer a larger shift from the Auger energy. To understand the reasons look at the results of Table VI, where we give the expansion coefficients of $\chi^l_{\beta,\mathbf{k}}$ with respect to the eigenvectors of the projected $\hat{F}_\beta$ classified according to their dominant character and eigenvalue. These results show that among the eigenvectors of a given type the most important one for the expansion of $\chi^l_{\beta,\mathbf{k}}$ is that

TABLE VI. Modulus of the expansion coefficients (a_j) of three LS orbitals, with respect to the basis set of the eigenvectors of the projected $\hat{F}_\beta$, classified according to their eigenvalue (ε_j). Note that $j=s,p,d$ indicates the dominant character of the eigenvector and c_j gives the position of its major component, while ε_k gives the energy of the Auger electron in the three states. Directions of $\mathbf{k}$ have been chosen in which all the components of the basis sets contribute. All the quantities are given in atomic units.

Auger electron energy	ε_s	a_s	c_s	ε_p	a_p	c_p	ε_d	a_d	c_d
				$^1\Sigma^+(3\sigma^{-1}3\sigma^{-1})$					
$\varepsilon_k=22.069$	4.485	0.039	F	5.074	0.078	F			
	18.792	0.683	F	7.519	0.085	F			
	23.462	0.409	F	38.993	0.180	F			
	45.068	0.053	F	74.304	0.072	F			
	1.298	0.007	Li	0.778	0.009	Li			
	9.325	0.074	Li	12.714	0.258	Li			
	34.008	0.164	Li	31.103	0.572	Li			
	107.990	0.040	Li						
				$^1\Pi(3\sigma^{-1}1\pi^{-1})$					
$\varepsilon_k=22.807$				8.800	0.007	F	34.490	0.492	F
				24.817	0.437	F	124.475	0.110	F
				57.749	0.055	F	330.157	0.064	F
				118.645	0.035	F			
				4.234	0.066	Li	46.602	0.449	Li
				14.113	0.301	Li	156.989	0.147	Li
				44.402	0.240	Li			
				125.593	0.084	Li			
				$^1\Delta(1\pi^{-1}1\pi^{-1})$					
$\varepsilon_k=23.888$							11.184	0.030	F
							23.896	0.788	F
							48.430	0.038	F
							94.320	0.032	F
							12.488	0.111	Li
							27.788	0.753	Li
							60.796	0.153	Li
							136.572	0.087	Li

TABLE VII. Values of the absolute (W_n^{abs}) and relative (W_n^{rel}) Auger transition rates for the LiF molecule calculated using our method with two scattering basis sets defined in Table V, and compared with the corresponding values ($\tilde{W}^{abs}$) and ($\tilde{W}^{rel}$) given in Refs. 5 and 27 and with the experimental quantities (W_{exp}^{rel}) (Ref. 26) for various decay states. Note that the experimental value of the total Auger rate has not been clearly determined. The absolute rates are given in 10^{-3} a.u.

State	W_1^{abs}	W_1^{rel}	W_2^{abs}	W_2^{rel}	$\tilde{W}^{abs}$	$\tilde{W}^{rel}$	W_{exp}^{rel}
1 $\pi_+\pi_-$ $^1\Sigma^+$	0.6206	0.3374	0.6232	0.3387	0.3845	0.17	0.27
2 $4\sigma 4\sigma$ $^1\Sigma^+$	0.7356	0.4000	0.7315	0.3975	0.7439	0.33	0.32
3 $3\sigma 4\sigma$ $^3\Sigma^+$	0.2358	0.1282	0.2363	0.1284	0.7643	0.34	0.07
4 $3\sigma 4\sigma$ $^1\Sigma^+$	0.6467	0.3516	0.5598	0.3042	0.0675	0.03	0.17
5 $3\sigma 3\sigma$ $^1\Sigma^+$	0.8866	0.4820	0.8902	0.4838	0.3435	0.15	0.21
6 $4\sigma\pi_+$ $^3\Pi$	0.0030	0.0017	0.0030	0.0017	0.0066	0.003	0.02
7 $4\sigma\pi_+$ $^1\Pi$	1.8178	0.9883	1.8184	0.9882	2.2505	0.98	0.91
8 $3\sigma\pi_+$ $^3\Pi$	0.4934	0.2683	0.4934	0.2681	1.4714	0.64	0.20
9 $3\sigma\pi_+$ $^1\Pi$	1.1801	0.6416	1.1819	0.6423	0.1436	0.06	0.42
10 $\pi_+\pi_+$ $^1\Delta$	1.8393	1.0000	1.8401	1.0000	2.2842	1.00	1.00
W_{tot}	8.4590		8.3779		8.4600		

having its eigenvalue closest to the Auger energy, while the coefficients of the other eigenvectors distribute quite symmetrically around the dominant one. Therefore we can generalize our conclusions, drawn from the atomic case, by saying that the variational stability of W_β corresponds to the presence in each type of basis functions of eigenvectors of the projected $\hat{F}_\beta$ having eigenvalues sufficiently close to the Auger energy. Note as a characteristic feature of our method that when the scattering basis set is not adequate to the problem, the plot of W_β as a function of the distance from the Auger energy does not exhibit a minimum, and this fact signals the need to improve the quality of the representation.

Finally in Table VII we compare the Auger rates, calculated using our method with those obtained by the authors in Ref. 5 with the experimental values.[26] In these results we can stress the following points.

(1) Using a LS wave function for the outgoing electron we have significantly improved our previous results[5] with respect to the experimental values. In particular, for transitions 3 and 4 the error has been reduced from a factor of ~ 5 to a factor of ~ 2 obtaining also the correct ratio between the two values, for transition 8 from a factor of ~ 3 to about 30%, and for transition 9 from a factor 7 to about 50%. With regards to transition 6, the relative value, which is very small, remains practically unchanged with respect to that in Ref. 5, but in this case the experimental value is about of the same order of magnitude as that for the forbidden transition to the state $^3\Sigma^-(\pi_+^{-1}\pi_-^{-1})$: $W_{exp}^{rel}=0.01$. This means that to reproduce this result the inclusion of the effects due to the coupling between electronic and nuclear motion is essential. The only transition for which the new relative decay rate differs from the experimental value more than in Ref. 5 is that relative to the state $^1\Sigma(3\sigma^{-1}3\sigma^{-1})$. However, we observe that such a state is the analog of the $^1S(2s^{-1}2s^{1-})$ for the neon atom, and, in fact, the absolute decay rate we have obtained is of the same order of magnitude as that for the atomic transition; therefore, we conclude that our value is a correct estimate of the Auger decay rate obtainable using an independent-particle approach, the discrepancy with respect to the experimental result being due mainly to correlation effects.

(2) Comparing the values obtained using two different basis sets, we observe that our results are not too sensitive to the quality of the basis set used, provided that it guarantees the variational stability of W_β. Finally, we point out that as far as the total Auger decay rate is concerned, our result differs by less than 1% from that obtained using an orthogonal plane wave for the outgoing electron.

V. CONCLUSIONS

In this paper we have proposed a method that for the limit of an independent-particle description of the states and making use of expansions in terms of discrete basis functions both of the orbitals and of the potential can be easily applied to the study of the Auger effect in molecules.

The results obtained in our test calculations on the neon atom show that using our method one can reproduce very well results obtained by means of numerical techniques, the application of which to molecular problems would present enormous difficulties.

An accurate prediction of the experimental Auger rates requires the inclusion of the correlation effects and also, in several cases, of the coupling between electronic and nuclear motion. However, as a preliminary step in many molecular problems it is useful to have an accurate estimate of the best values of the transition rates obtainable using an independent-particle approach. To this end, we have proposed a simplified version of our method that satisfies this need and furthermore has allowed us to obtain a very satisfactory reproduction of the experimental Auger spectrum of the LiF molecule.

ACKNOWLEDGMENTS

We thank Professor F. Bassani for helpful conversations and constant encouragement and Professor T. O. Woodruff for suggestions concerning the manuscript. One of us (S.S.) wishes to acknowledge the financial support granted by E.N.I. (Ente Nazionale Idrocarburi) within the "Perfezionamento in Scienze Molecolari Applicate" at Scuola Normale Superiore.

[1]T. Åberg and G. Howat, in *Corpuscles and Radiation in Matter I,* Vol. 31 of *Handbüch der Physik* (Springer, Berlin, 1982), and references therein.
[2]K. Faegri, Jr. and H. P. Kelly, Phys. Rev. A **19**, 1649 (1979).
[3]M. Higashi, E. Hiroike, and T. Nakajima, Chem. Phys. **68**, 377 (1982).
[4]V. Carravetta and H. Ågren, Phys. Rev. A **35**, 1022 (1987).
[5]R. Colle, S. Simonucci, and T. O. Woodruff, Phys. Rev. A **38**, 694 (1988).
[6]C. Liegener, Chem. Phys. Lett. **106**, 201 (1984), and references therein.
[7]M. Cini, F. Maracci, and R. Platania, J. Electron Spectrosc. Relat. Phenom. **41**, 37 (1986).
[8]H. Ågren and H. Siegbahn, Chem. Phys. Lett. **72**, 498 (1980).
[9]O. M. Kvalheim and K. Faegri, Jr., Chem. Phys. Lett. **67**, 127 (1979).
[10]D. J. Ernst, C. M. Shakin, and R. M. Thaler, Phys. Rev. C **8**, 46 (1973).
[11]T. M. Rescigno, C. W. McCurdy, Jr., and V. McKoy, Phys. Rev. A **11**, 825 (1975).
[12]T. M. Rescigno, C. W. McCurdy, Jr., and V. McKoy, Chem. Phys. Lett. **27**, 401 (1974).
[13]T. M. Rescigno, C. W. McCurdy, Jr., and V. McKoy, Phys. Rev. A **10**, 2240 (1974).
[14]R. Colle, A. Fortunelli, and S. Simonucci, Nuovo Cimento D **9**, 969 (1987).
[15]R. Colle, A. Fortunelli, and S. Simonucci, Nuovo Cimento D **10**, 805 (1988).
[16]R. Colle and S. Simonucci, Nuovo Cimento (to be published).
[17]R. K. Nesbet, *Electron-Atom Scattering Theory* (Plenum, New York, 1980).
[18]A. W. Fliflet, D. A. Levin, M. Ma, and V. McKoy, Phys. Rev. A **17**, 160 (1978).
[19]A. W. Fliflet and V. McKoy, Phys. Rev. A **18**, 1048 (1978).
[20]W. Kohn, Phys. Rev. **74**, 1763 (1948).
[21]W. H. Press, B. P. Flannery, S. A. Teukolsky, and W. T. Vetterling, *Numerical Recipes* (Cambridge University Press, Cambridge, 1986), p. 547.
[22]H. P. Kelly, Phys. Rev. A **11**, 556 (1975).
[23]H. Koerber and W. Mehlhorn, Z. Phys. **191**, 217 (1966).
[24]U. Gelius, S. Svensson, H. Siegbahn, E. Basilier, A. Faxalv, and K. Siegbahn, Chem. Phys. Lett. **28**, 1 (1974).
[25]F. B. Van Duijneveldt, IBM Res. J. **945**, No. 16437 (1971).
[26]M. Hotokka, H. Ågren, H. Aksela, and S. Aksela, Phys. Rev. A **30**, 1855 (1984).
[27]Note that the value of $\tilde{W}^{\text{rel}}$ reported in Ref. 5 for the transition rate to the state $^1\Sigma(3\sigma^{-1}4\sigma^{-1})$ is wrong, the correct one being given in Table VII.